CAAP Quarterly Report

Date of Report: *January 7, 2015*

Contract Number: *DTPH5614HCAP04*

Prepared for: *Dr. James Merritt, PHMSA-DOT*

Project Title: *Optimized Diagnosis and Prognosis for Impingement Failure of PA and PE Piping Materials*

Prepared by: *University of Colorado-Denver, Arizona State University*

Contact Information: *Dr. Yiming Deng and Dr. Yongming Liu*

For quarterly period ending: *January 10, 2015*

Business and Activity Section

(a) Generated Commitments

Pipeline infrastructure and its safety is critical for the recovering of U.S. economy and our standard of living. Statistics from U.S. Department of Transportation (DOT) and Gas Technology Institute (GTI) show the decline in use of steel and cast iron piping materials is significant in recent years and the increase in pipeline system size is largely due to plastic pipe installations. However, failure inevitably occurs in plastic piping materials and impingement failure is caused by high localized stress concentration combined with defects and inclusions. Previous research efforts were mainly focusing on PE materials, efficient and effective impingement damage diagnosis and prognosis of various types of new plastic piping materials still remain unaddressed and challenging. The proposed research will fundamentally understand and characterize the failure modes and associated material behaviors for modern plastic piping materials. The proposed optimized diagnosis and prognosis approaches will thoroughly investigate and compare the dominating PE materials (make up nearly 97% of current plastic pipes) and the emerging PA pipes that can operate at much higher pressures and be installed using existing PE tools and techniques. If successful, this study can help to effectively maintain and improve the reliability of pipeline systems, and ultimately reduce the environmental consequences because of a pipeline catastrophic failure.

The overall objectives of the proposed research are two-fold: optimized diagnosis-find existing impingement damage at the earliest stage before it becomes failure critical in PE and PA materials, conduct comprehensive comparison studies to identify the differences in micro-cracking mechanism between these two materials; and optimized prognosis - accurately predict the remaining strength and RUL of PE and PA components through mechanical modeling and experimental investigations.

The eighteen-month effort will establish a framework composed of both physical (CU) and mechanical modeling (ASU) with optimized parametric studies both numerically and experimentally, and models validation during the first project year (month 1 to month 12). A thorough anomaly detection, characterization and sensitivity analysis for both optimized diagnosis and prognosis algorithms will be carried out in the second project year (month 13 to month 16). Building upon achieving these research milestones, a model-assisted detection and prediction framework with the integrated diagnosis and prognosis capabilities will be realized and tested in field at the last phase of this project (month 16 to month 18). The specific technical objectives are addressed through the

following two major research tasks, each has three subtasks:

Task 1 focuses on the sensing physics modeling of impingement failure diagnosis and experimental investigation assisted by model-based inversion techniques. Three subtasks are proposed: (1.1) element-free Galerkin's method (EFG) development for the electromagnetic modeling of arbitrary and micro-scale crack initiation and propagation due to impingement; (1.2) model-based inversion for ultra-fast impingement failure reconstruction and sensing assisted by compressed sensing techniques; (1.3) demonstration of optimized diagnosis capabilities using electromagnetic diffraction tomography array.

Task 2 focuses on the mechanical modeling of impingement failure and experimental investigation. Three subtasks are proposed: (2.1) extended finite element method (XFEM) and cohesive zone modeling (CZM) for the crack initiation and propagation simulation; (2.2) experimental investigation of impingement effect on the failure of investigated materials; (2.3) parametric study and sensitivity analysis for the optimized prognosis algorithms.

(b) Status Update of Past Quarter Activities

Task 1- Sensing physics modeling of impingement failure diagnosis and experimental investigation assisted by model-based inversion techniques for PE and PA material

Subtask 1.1 Physics modeling for imaging of PE and PA piping materials

Polyethylene (PE) is a cost effective solution for a broad range of piping problem in a variety of industries. It has been tested and proven effective for above ground, surface, buried applications. High-density polyethylene pipe (HDPE) can carry portable water, wastewater, chemicals, and compressed gases. Polyethylene is strong, extremely tough and very durable. Since it is a plastic material, polyethylene does not rust, rot or corrode, this will lower the life cycle costs.

PA11 is a material of choice for corrosion free, aggressive hydrocarbon transport system. PA11 thermoplastic material has been used across the entire oil and gas value chain extensively, for cost-effective non-metallic piping systems. PA11 provide a better value compare to steel pipe. It has lower total installation cost, lower lifetime maintenance, and comparable performance. According to a brochure from Arkema, Inc., PA11 also shows excellent resistance to slow crack growth.

Simulation study is an important way to assist experimental studies and sensor development via optimization of critical parameters. In this 5th quarter, we continued the effort of developing a FEKO model as well as the Element-free Galerkin model to assist the experiment scanning and understand the imaging physics for both PE and PA11 materials. The goal of the simulation is to study the electric field distribution along the target to verify the experiment results.

The results in previous quarters showed that the size of the probes that we used in experiment have the abilities to achieve high resolution images. In this quarter, we further studied PE and PA11 material properties using 3D models with 1D linear array and 2D scanning array. For the experiment, the focus was to retrieve amplitude and phase of the reflected microwave to map the physical properties of the surface and subsurface of the material, then compare with the digital image correlation (DIC) results obtained at ASU team. The simulation model will focus on the radiation field of each scanning probe tips to verify if the scanning array has the ability to identify the different materials.

First, we compared the electric field of PA and PE materials with linear array in a validated 3D model developed in Q1 to Q4. The design of the array showed in Fig. 1. The diameter of the hole or artificial damage is 5 mm. Both PE and PA plate have the same size of 340 mm x 486 mm x 8 mm, which is the same as the actually testing sample in the CU LEAP lab. We further validated the conclusion we reached at the end of Q4 that since PA has slightly higher dielectric constant value compare to PE material, we expect to see that PE material has higher electric field around the probe tips than PA material. Because the simulation results showed the field that radiated around the tip. The higher dielectric constant means the material stores more energy and more response with same shape and voltage. PA material should have

more reflection compare to PE material, which means PE material will have more field concentrated around the probe tip than PA material.

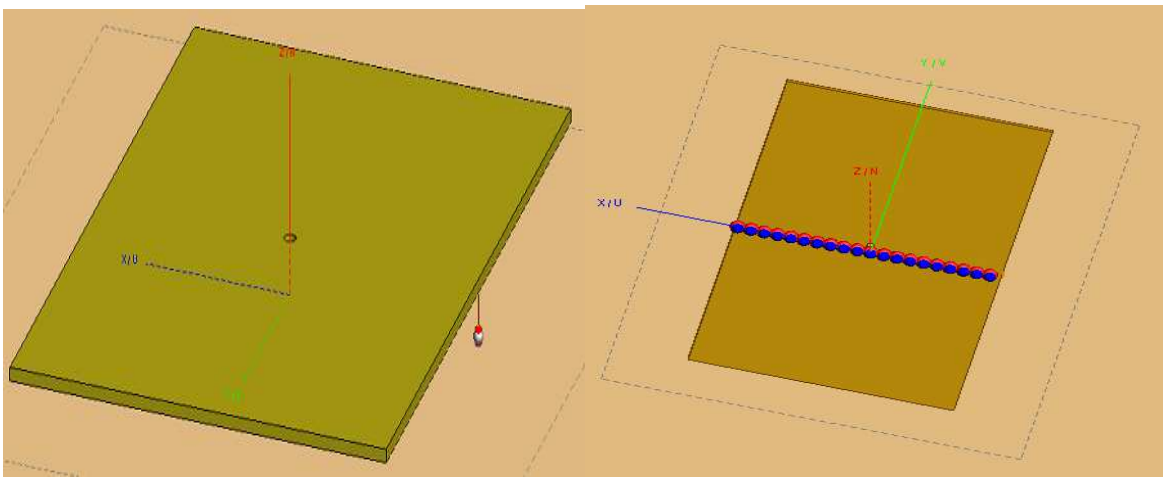

Fig. 1 Linear scanning array for both PE and PA plate model

Fig. 2 shows the simulation results of PA and PE material with circular pipe shaped scanning array. As expected, electric field for PA is lower than for PE. This can help us to identify the materials during the experiment.

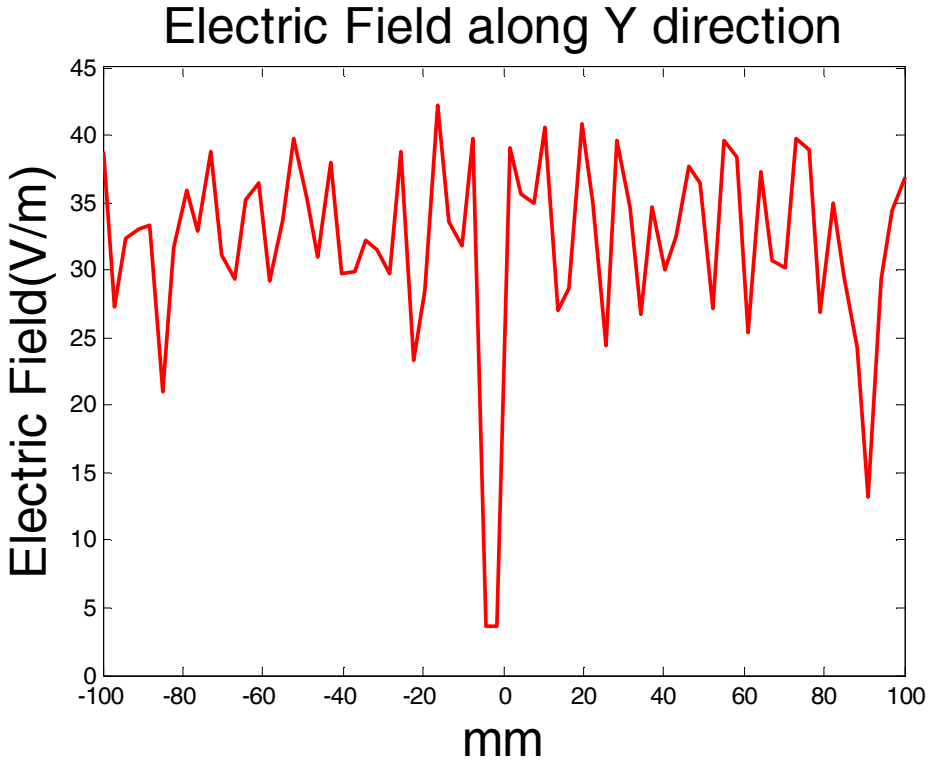

(a)

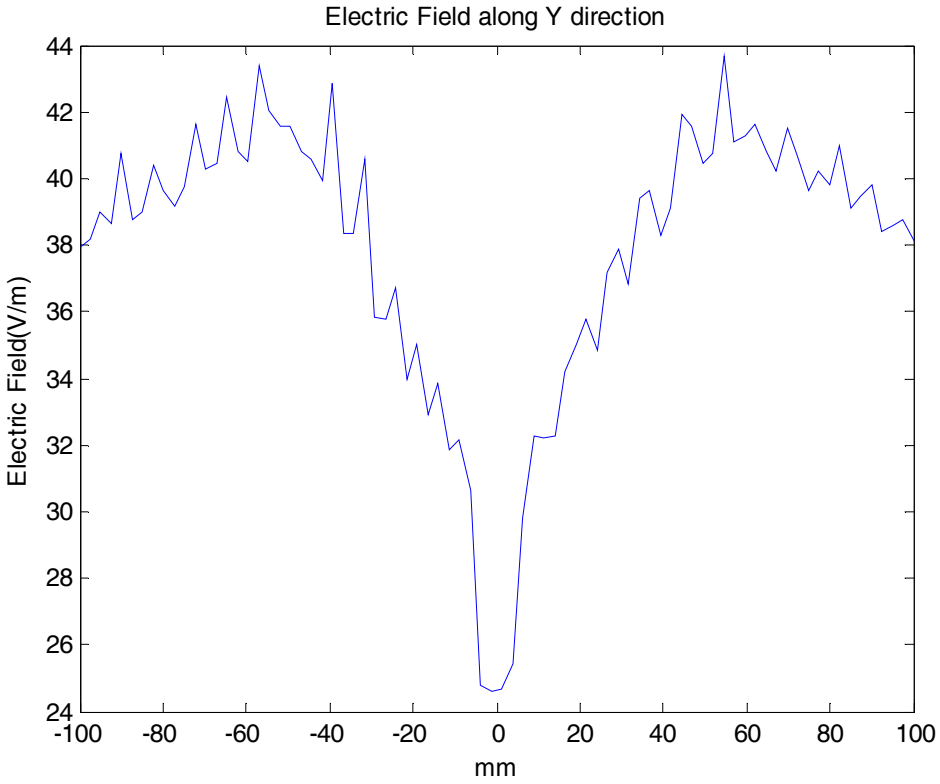

(b)

Fig. 2 Comparison of near-field microwave responses of single hole damage and linear scanning array for (a) PE and (b) PA-11 materials. Larger signal (E-field intensity) is expected from PA-11 sample.

Next, a two-dimensional (2D) scan is simulated in this well-developed 3D model and the exemplary imaging result is shown in Fig. 3. Subsurface square damage are clearly identified and segmented from the image data, which demonstrated the detection capability of the developed sensor array for PE and PA materials. The extracted 1D signals are shown in Fig. 4, in which the PA materials had higher damage responses than PE materials, which means that the damage will be more sensitive or easier to be detected for PA using the same diagnosis technique developed under this project.

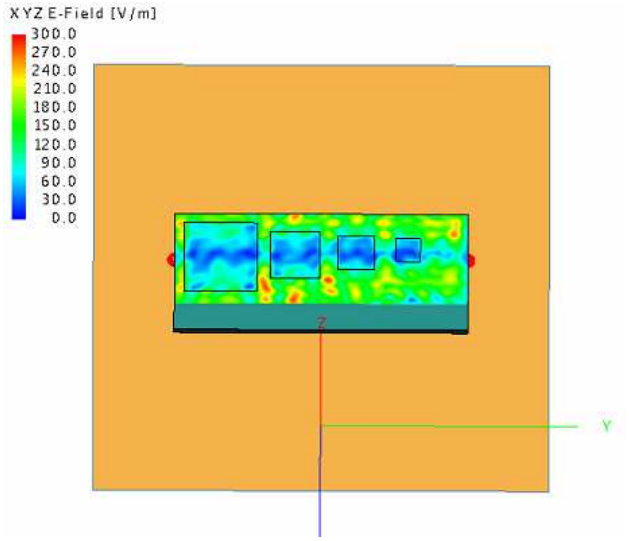

Fig. 3. 2D imaging results for damage detection of PA-11 sample.

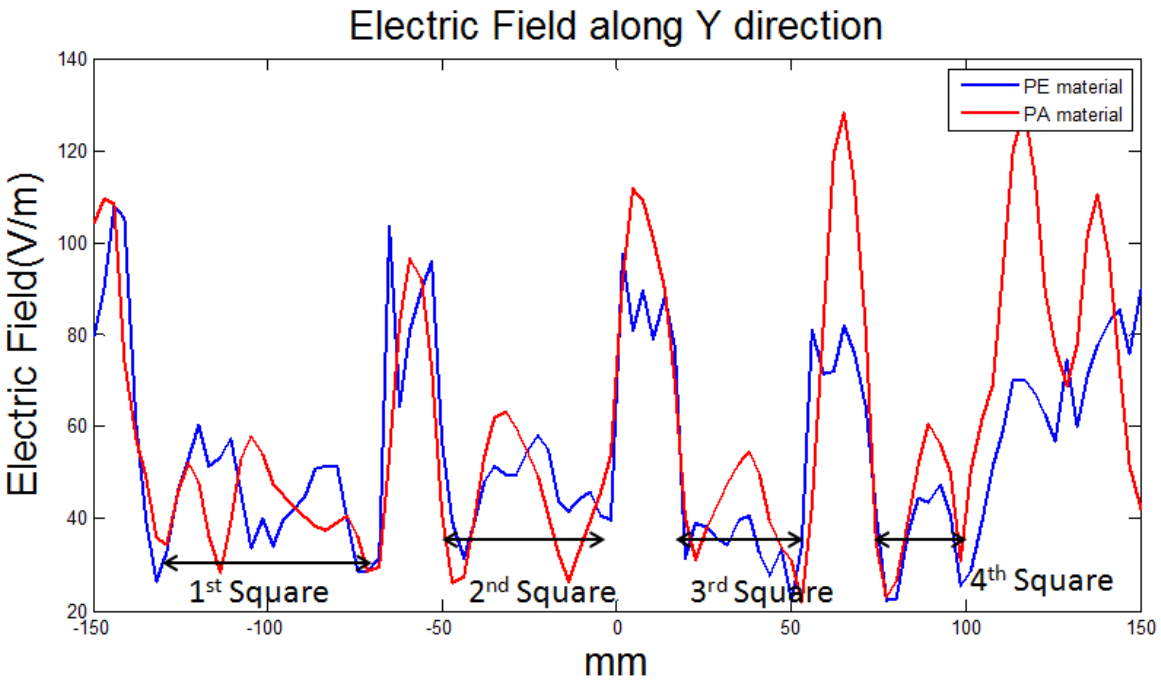

Fig. 4. Comparison of 1D PE and PA materials responses to square damage with different sizes.

Subtask 1.2 Imaging optimization and comparison with DIC results

In Q5, we performed near field microwave scan of both full specimens (without any hole) and notched specimens (specimen with hole) from industry collaborators. The resulting image of four notched specimens is shown below in Fig. 5.

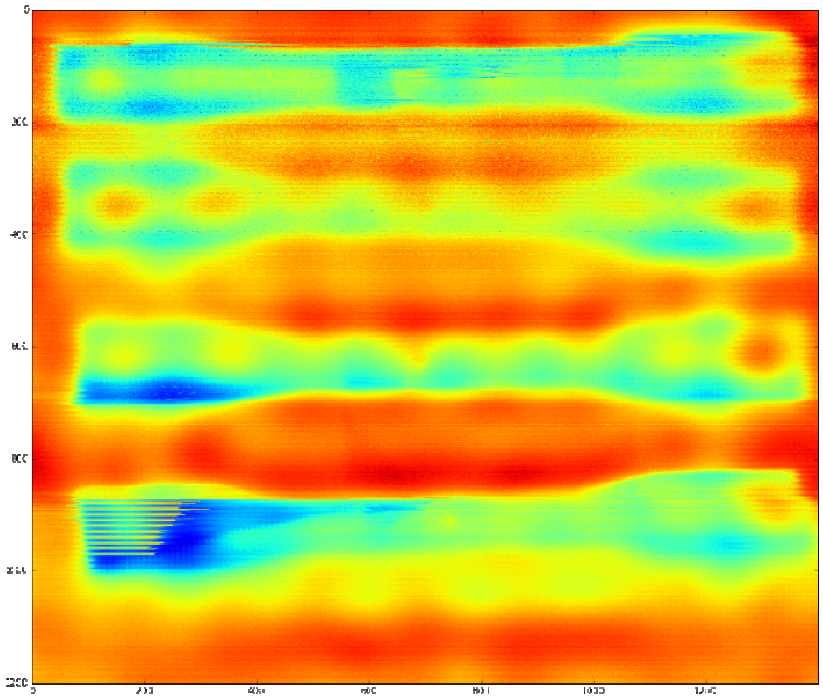

Fig. 5. Near-field microwave scan of notched specimens

As the image shown above, the four specimens from top to the bottom are 70%, 50%, 30%, 0% of maximum value of displacement at fracture to which the specimens are elongated, respectively.

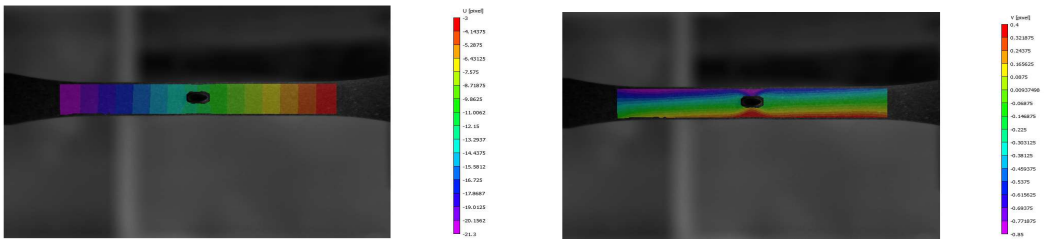

(a).U (mm) displacement (b).V (mm) displacement

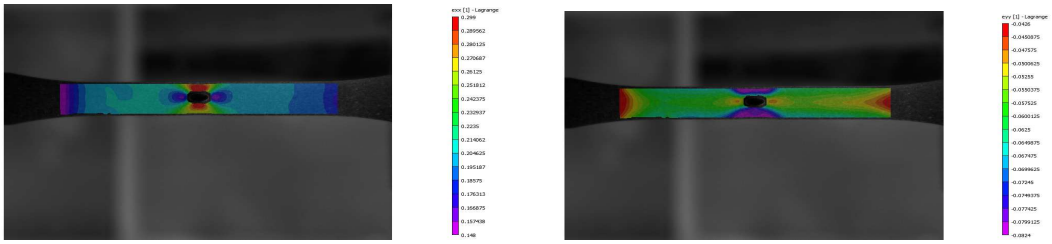

(c).local strain - X (exx) (d). local strain - Y (eyy)

Fig. 6 tensile images of 0.7 notched specimens from Arizona State University

Fig. 6 shows the tensile test data notched specimens elongated at 70% of maximum value of displacement at fracture. A preliminary comparison has been shown in Fig. 7. As we can see in the image, both of the two image display a changing value around the hole. Also, they are both centrosymmetric.

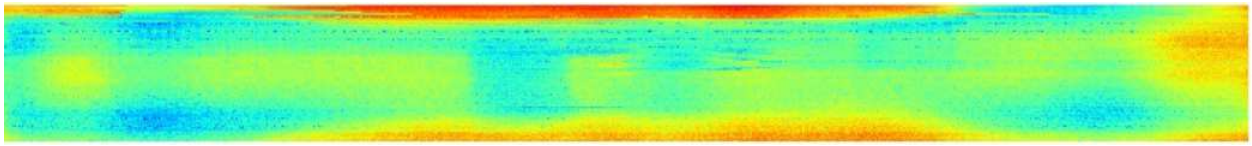

(a)

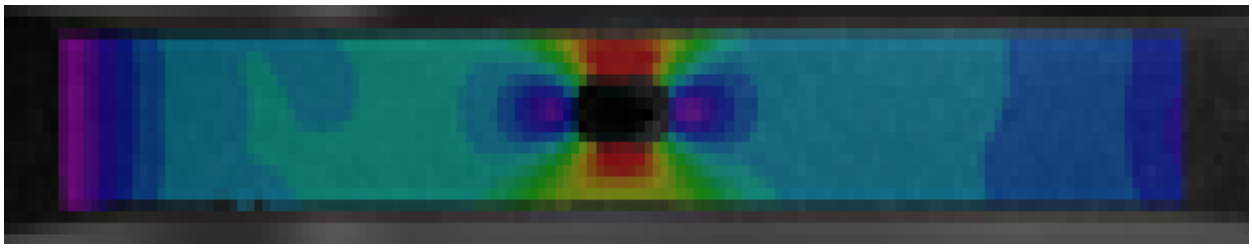

(b)

Fig.7 Preliminary comparison of NS 0.7: (a) NFMM results and (b) DIC results

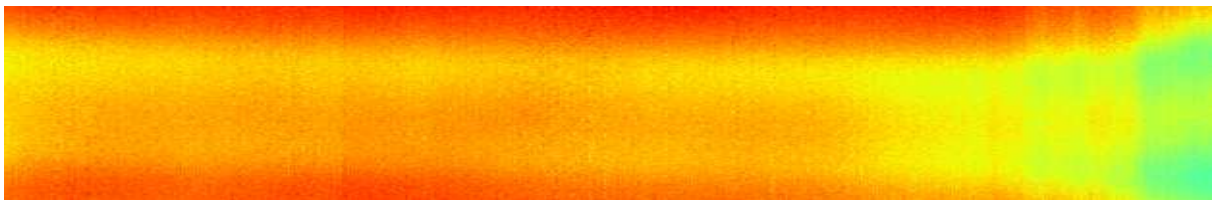

(a)

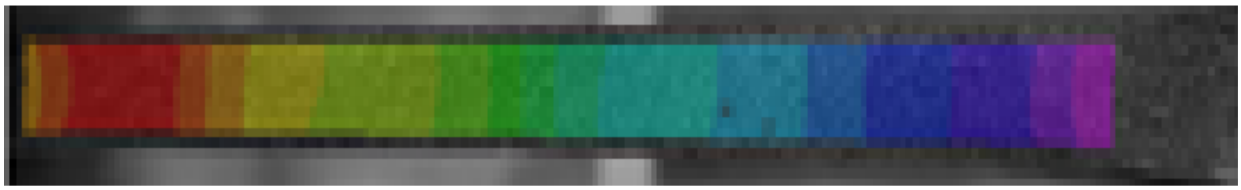

(b)

Fig.8 Preliminary comparison of FS 0.5: (a) NFMM results and (b) DIC results

For full specimen (without any hole) shown in figure 8, we can see that none of them are centrosymmetric. The values in two images are both changing smoothly. Further comparison with quantitative metrics that will analyze the similarity between the imaging results from two modalities will be developed in the next quarter.

Meanwhile, the multi-channel sensing prototype is being developed. In this 5th quarter, we designed and fabricated the multi-channel scanning sensor tip the control circuit for the multi-channel scanning sensor for improving the scanning speed. A control circuit also has been designed same setup as the current experiment. The innovative design of the control circuit shows in Fig. 9(a). Compared with the current experiment, shown in Fig. 9(b), the control circuit compresses the directional coupler, RF to AC converter and data collection together to perform the same function. The control circuit uses a microcontroller to control the input and receive signal. There is no connection between data processing and receiving signal in the control circuit design, which will reduce the scanning time.

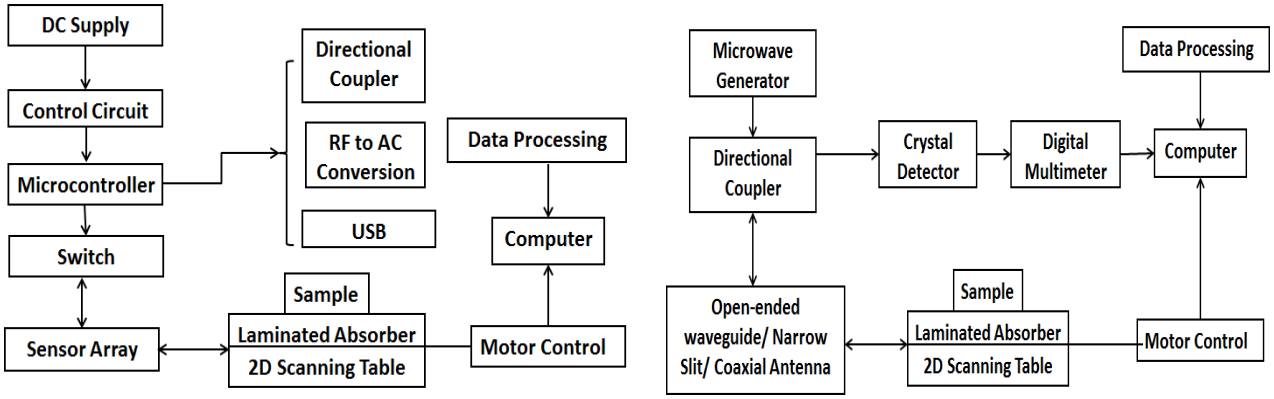

(a) Improved design with Control circuit (b) Current experiment design

Fig. 9. Design comparison of control circuit and current experiment setup

Task 2-Mechanical modeling on impingement failure

Task 2 focuses on the mechanical modeling and comparison of PA and PE materials. Two major subtasks are performed: 1) preliminary development of a coupled diffusion fracture simulation framework to consider the effect of hydrogen diffusion on the mechanical performance of PE and PA materials; 2) experimental testing for the investigation of impingement effect on the material failure strength and strain. Both subtasks are ongoing and the current report mainly focuses on the experimental testing part.

Subtasks 2.1 Experimental investigation of impingement effect on material strength

1.0 OBJECTIVE

The major research objectives of the project are:

- Simulate the pipe crack propagation using XFEM and investigate the effect material properties, pressure, and crack geometries to the final failure.

- Design of experiments and response surface method to construct a function between the load carrying capacity with respect to design variables.
- Perform probabilistic reliability analysis considering the uncertainties

In the last quarter report, tensile testing methodology and results for PA 11 samples with a hole at its center and also specimen without hole were reported along with DIC images of each of the two specimens types that were elongated up to 30%, 50%, 70% of maximum elongation. The data was shared with CU, Denver for further investigation.
This particular report primarily encompasses the methodology and outcomes of the short term tensile testing of Polyethylene (PE) samples along with its strain maps obtained using Digital Image Correlation (DIC) technique and also the preliminary simulation results of Polyamide 11 (PA11) material performed in ABAQUS software.

2.0 INTRODUCTION

The testing of plastics includes wide variety of thermal, chemical and mechanical tests. This particular article reviews the standardized tensile testing method i.e. ASTM D638 along with the various practices adopted by engineers and scientists to test for the tensile properties of plastics. Tensile test embraces various procedures by which modulus, strength and ductility can be assessed. Generally, the term 'tensile test" means a test wherein a slender specimen is extended uniaxial at a uniform rate. Ideally, specimen should be slender with constant cross section across the gage length, free to contract laterally and expand longitudinally. Though this test was initially designed for testing metals, it was later adopted and adapted for testing plastics and polymers. In the case of plastics, the adaptation had to encompass for the visco-elastic behavior, probable anisotropy of the product. The deformation mechanism of polymers differs from that of metals. In most polymers, only about half of the work of plastic deformation is liberated as heat.
In case of metals, the plastic deformation results in relative change of orientations and positions of metal molecules. So, the large amount of stored integral energy of the polymers have many effects not seen in case of metals. One consequence is, when a unconstrained polymer that has undergone plastic deformation is heated, it will contract toward its original length. The ultimate tensile strength of most of the plastics ranges from 50-80Mpa. The mechanical behavior of polymers is a function of temperature as well as time. So, the data based on short term test have possibility of misinterpreting the results of tested polymers in a design application involving long-term loading conditions.

2.1 Polyethylene material

Polyethylene (PE), light, versatile synthetic resin made from the polymerization of ethylene. Polyethylene is a member of the important family of polyolefin resins. It is the most widely used plastic in the world, being made into products ranging from clear food wrap and shopping bags to detergent bottles and automobile fuel tanks. [1]

PE materials are used in pipelines due to its chemical inertness, non-corrosive nature and long term durability offers outstanding service life, with conservative estimates standing at 100+ years. [2] So, PE pipeline finds application in transporting water and gas where pressure containment and structural integrity is considered critical for the lifetime of the pipeline since system failure can result in flood, explosion, fire and loss of life resulting in costly litigation and damages.

3.0 FACTORS AFFECTING TESNISLE TEST DATA

Plastics are visco-elastic materials, in which deformation can be dependent on temperature as well as time. Probable anisotropy in the plastic can affect the tests [3].

Viscoelasticity: The time dependence of the deformation of visco-elastic materials can be attributed to rate at which stress is applied. The temperature dependence will depend on the properties of plastic itself which are different for amorphous, crystalline and semi-crystalline [3][4]. As a result, during the tensile test the specimen may distort near grips and clamping forces may relax with passage of time. The subsequent force displacement curves obtained from the tests performed would have time dependence as well as effect of strain rate incorporated. To this effect, Reis et al proposed a model and validated them to evaluate mechanical tensile properties at different strain rates for HDPE [5]. Serban et al reported that for semi crystalline polymers temperature & strain rate changes affects Young's modulus the most with minimal impact on tensile strength [6].

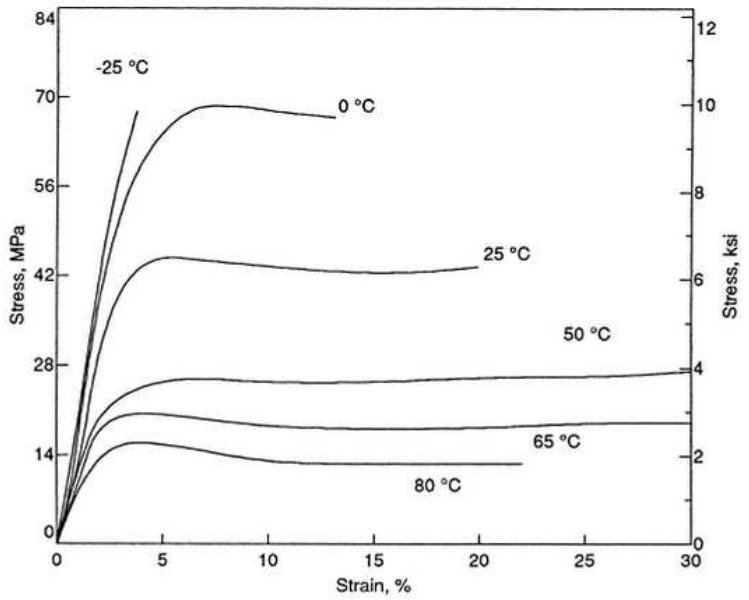

Fig. 1 Influence of Temperature on Stress- Strain curves, Stain rates have a similar effect [2]

Anisotropy: Due to anisotropic behavior of certain plastics, the specimens under investigation have a tendency to deform in irregular ways and may break at points other than those which have minimum cross-section. There are chances that failure takes place at the grips unless special precautions are taken. So, as a result of which the moduli and strength may be higher or lower than expected due to this anisotropy that may be introduced by flow geometry [7]. Recent work on this by Dyamenahalli0 et al in the characterization of shape memory polymers for tensile properties conclude that for anisotropic polymers which have discontinuous phase requires use of biaxial testing systems [8].

Specimen Preparation: One of the important parts of D638 is specimen preparation. Care should be taken to ensure all samples are prepared in exactly the same way. Because mechanical properties are sensitive to temperature and absorbed moisture, conditioning procedure for test specimen have been developed and defined in ASTM D618 & ISO 291. ASTM D638 has laid down specimen drawings with five types of dimensions depending on the desired thickness and testing conditions.

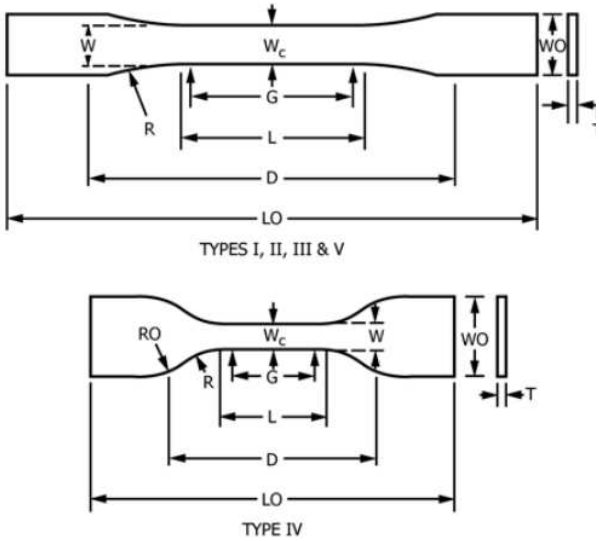

Dimensions (see drawings)	Type I
W—Width of narrow section[E,F]	13 (0.50)
L—Length of narrow section	57 (2.25)
WO—Width overall, min[G]	19 (0.75)
WO—Width overall, min[G]	...
LO—Length overall, min[H]	165 (6.5)
G—Gage length[I]	50 (2.00)
G—Gage length[I]	...
D—Distance between grips	115 (4.5)
R—Radius of fillet	76 (3.00)
RO—Outer radius (Type IV)	...

Fig 2. Dimension and shape Type 1 specimen from ASTM

3.0 EXPERIMENTAL PROCEDURE

3.1 Test specimen preparation.

Test specimens of ASTM Type 1 were used in the short term tensile testing. The material used for the testing is Polyamide 11. In order to introduce an impingement, holes were drilled at the mid-section of the specimen. The circular holes, which were of varying size and depth, were drilled by the NC Machining center as shown in Fig. 2. The maximum and minimum diameter of the hole were ¼'' & 1/8'' respectively. With regards to depth of the hole, it was either a through hole or a hole that was as deep as half of the specimen's thickness. Speckle pattern were created on each of the specimens for DIC strain measurements.

Fig. 3 Typical PE ASTM Type 1 specimen with speckle pattern.

4.2. Measurements

Tensile tests were performed on a universal testing machine (make; MTS Alliance 10/R) as presented in Fig. 3. The ultimate tensile strength, % elongation, yield strength (at 0.2% strain), and Young's modulus of each of the specimens at 0.2 in/min strain rate and 3.75'' gauge length was measured for each specimen. Strain measurements of each of the specimens tested were accomplished by optical technique, namely Digital Image Correlation (DIC). Images were captured using Lumenera Infinity 2 Camera. The captured images were analysed by commercial DIC tool Vic-2D.

Fig. 4 MTS Universal Testing Machine along with camera

4.3 Experiment order:

The testing includes parameters that would affect the mechanical property of PE and demonstrate the effects of impingement on the material. So, the variable parameters that are considered are size (diameter) and depth of the hole. The response parameters were Ultimate load, % elongation. Test matrix was prepared accordingly as shown in Table 1.

Specimen No.	Depth of impingement [a]	Diameter of impingement
N1	0	0
N2	0.12''	¼''
N3	0.12"	1/8''
N4	0.06"	¼''
N5	0.06"	1/8"

[a] Avg. thickness of specimen 0.12"

Table 1. Tensile test matrix

5.0 RESULTS AND DISCUSSION

A total of 5 experiments were conducted at two independent input variables as per designed plan. Experimental design matrix with measured data is presented in Table 1. The average Young's modulus and Yield Strength were found to be 165.35 ksi and 3.80 ksi respectively

The images were captured for optical strain measurements. DIC analysis was executed using Vic-2D software. However, the testing of PE specimen without hole i.e. N1 from Table 1 could not completed because the existing setup was not adequate in terms of its elongation limits, thus limiting the data obtained on failure elongation. Fig 5 shows the N1 specimen loaded onto the machine. Fig 6. A & B shows the curves obtained for tested specimens.

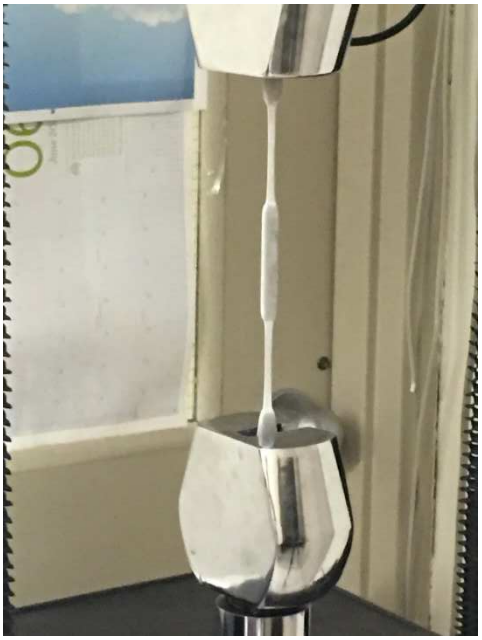

Fig. 5 N1 specimen loaded onto the MTS machine

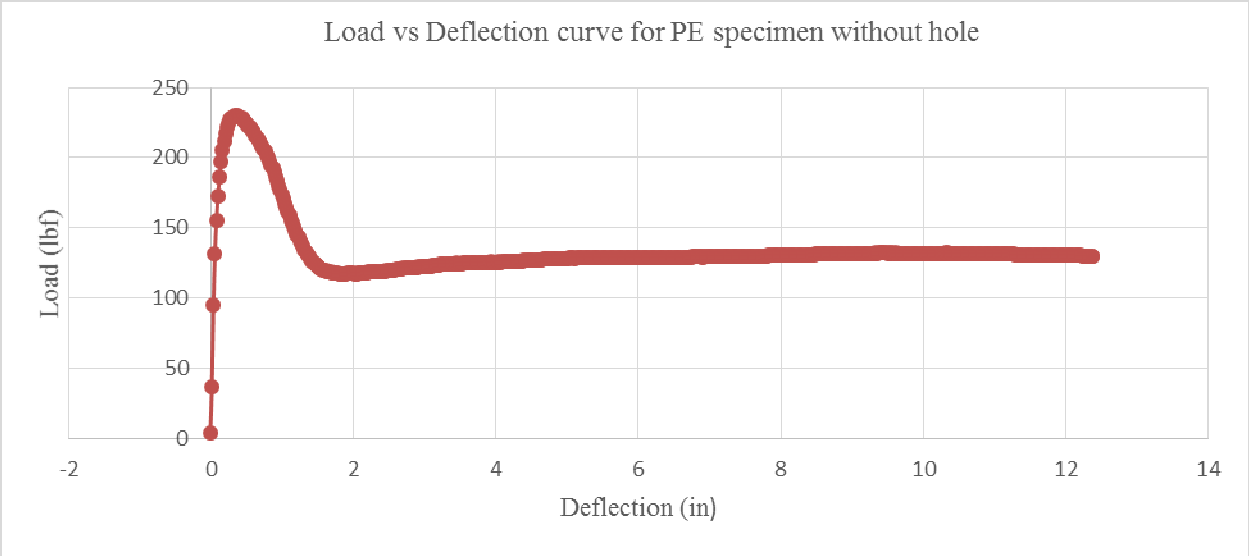

a)

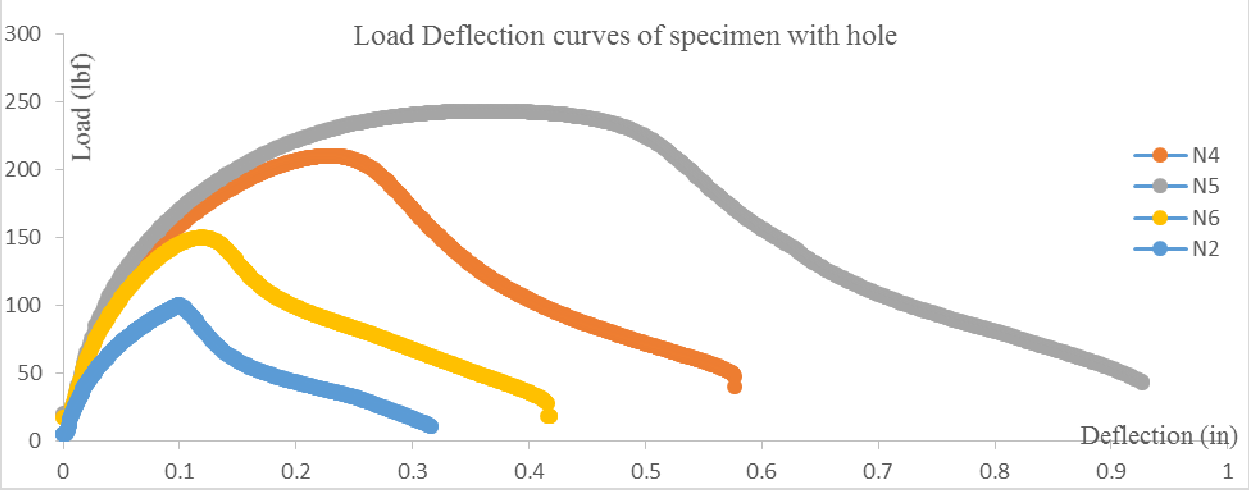

b)

Fig. 6 Load vs Extension curves for tested specimens

Specimen no.	Peak load(lbf)	% elongation
N1	245.321	-n/a-
N2	100.301	9.9
N3	150.116	11.18
N4	210.359	23.1
N5	243.343	36.7

Table 2. Results from ASTM D638 Tensile testing of PA 11

The PE material undergoes ductile fracture with long necking phase as seen in the graph. However, since the machine was not capable of testing N1 specimen entirely, the fracture strain and also the local strain at fracture data from DIC analysis could not be obtained.

Based on the results obtained, it is evident that any impingement on PE 11 material affects the strength and toughness of the material. Impingement has a direct impact on load bearing and ductility of the material. There is a reduction of over 50% in the peak load of the specimen with highest degree of impingement in terms of its size and depth. Similar trend can be observed in the ductility (% elongation) of the material wherein, there is a minimal elongation of impinged specimen. The graphs shown in Fig 6 a & b clearly indicate the trends for all the tested specimens. Moreover, the DIC strain maps in the subsequent sections will also further strengthened the observation.

5.1 DIC analysis of PE samples

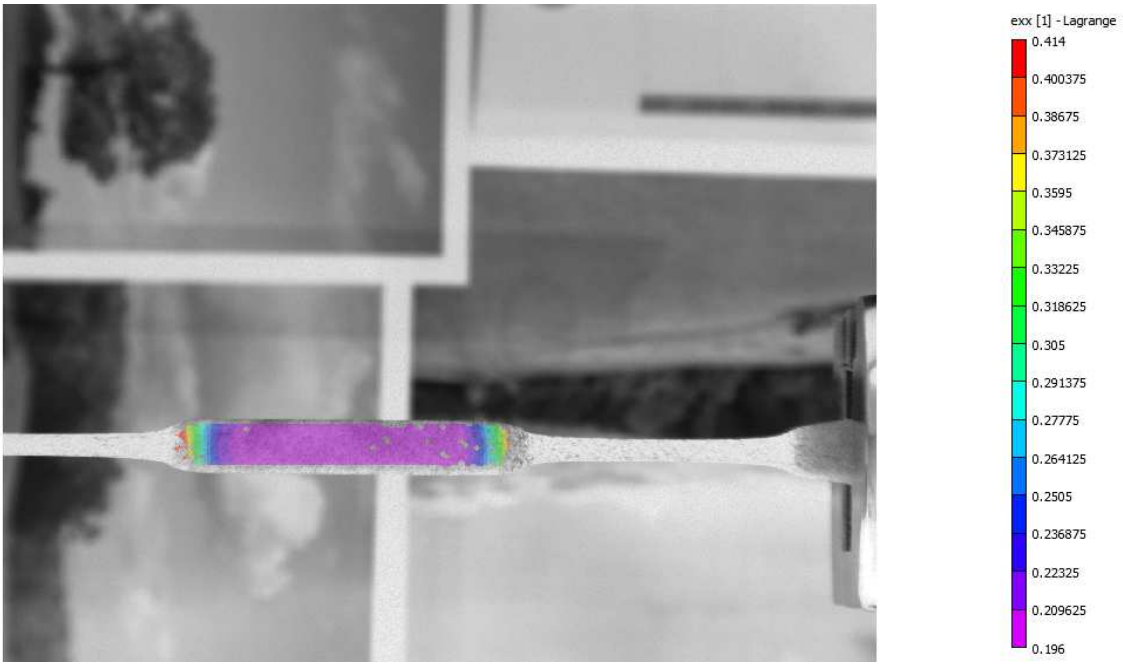

a) N1: (Max strain >0.414)

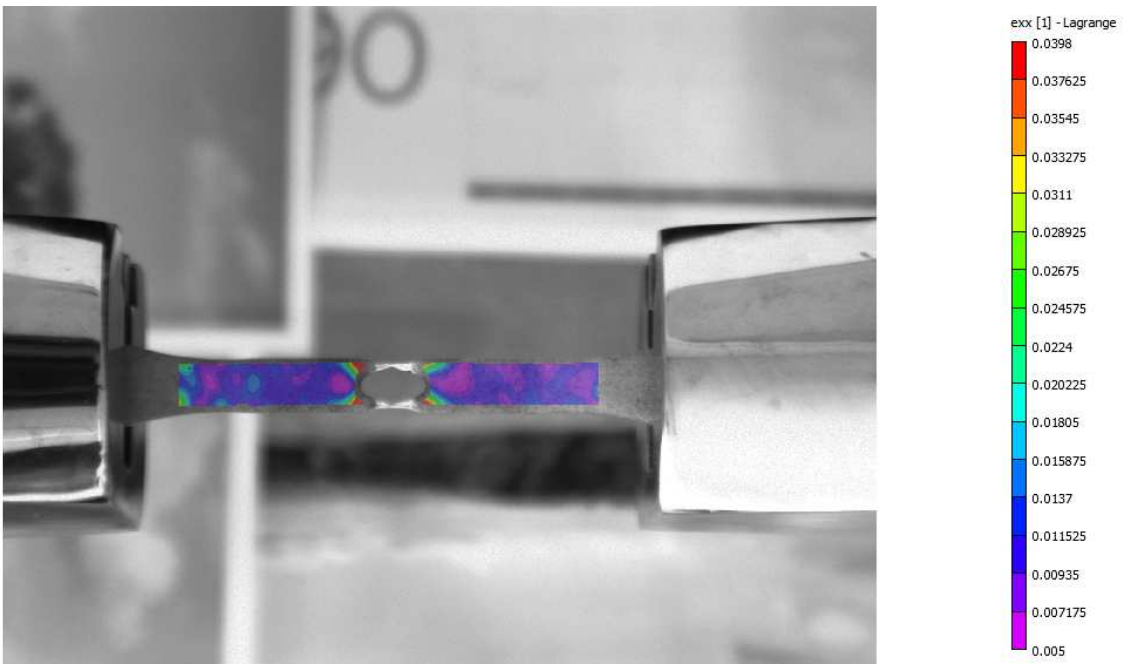

b) N2: (Max strain 0.0398)

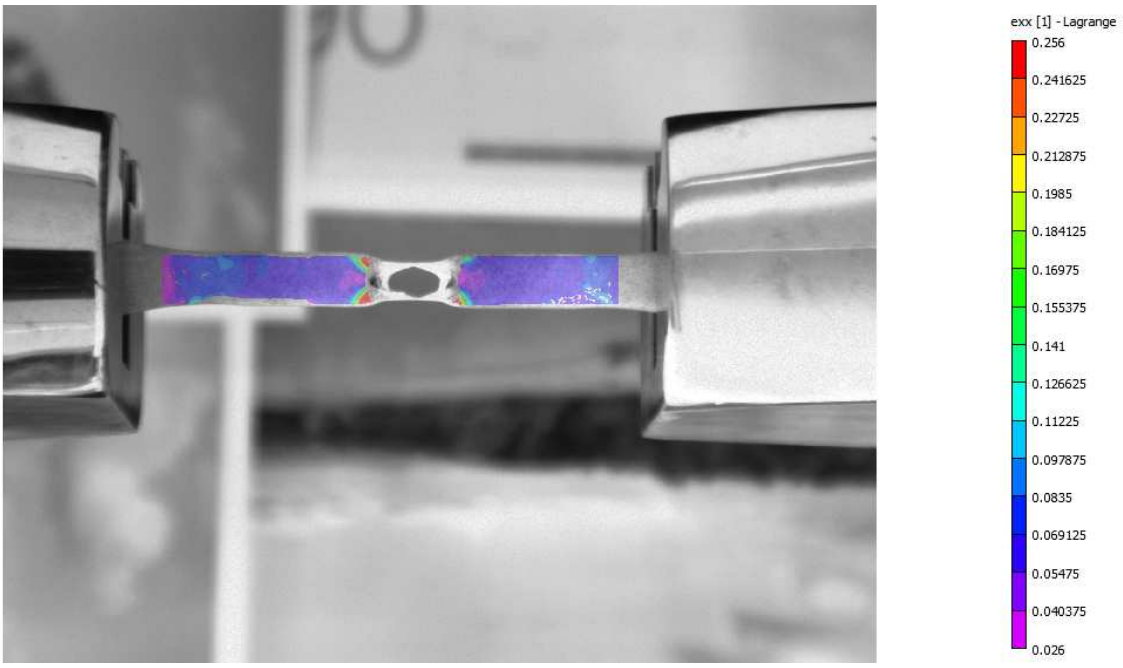

c) N3: (Max strain 0.256)

d) N4: (Max strain 0.204)

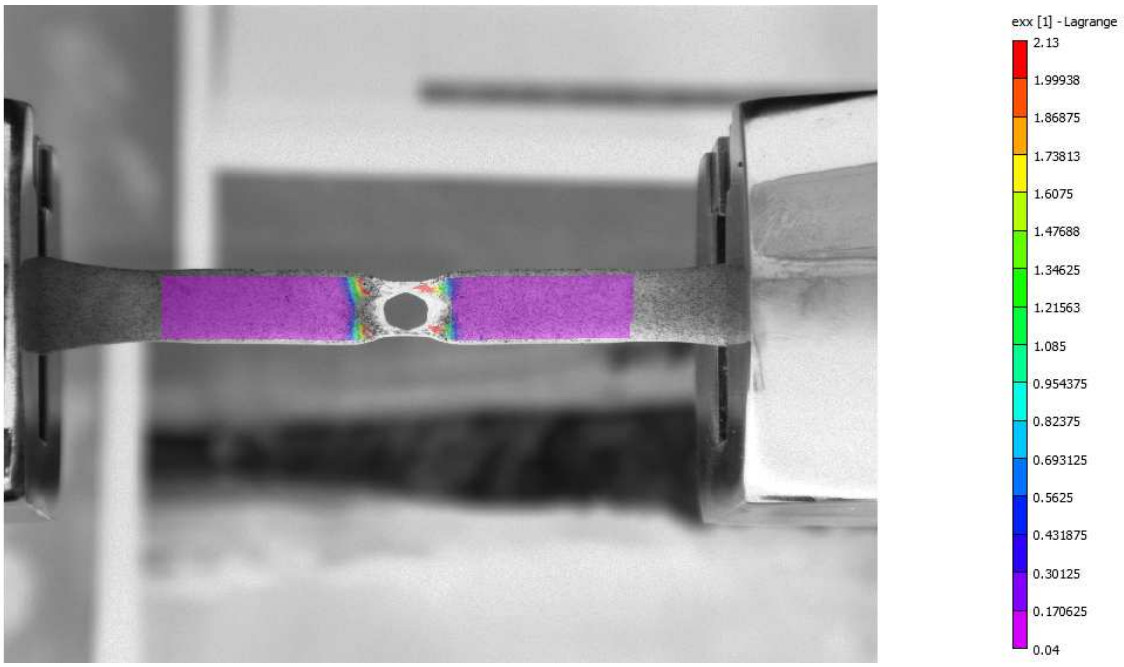

e) N5: (Max strain 2.13)

Fig. 7 Stain maps from DIC

6.0 NUMERICAL SIMULATION

A numerical elastic-plastic analyis of the tensile test specimen is being carried out to validate the numerical model built during intial phase of this project. The simulations are being carried out in ABAQUS/CAE software package.

The intial stage of simulations involved modelling the test speciemen (neglecting the grip supports) and meshing the part modelled. The next important step is material modelling. The experimental data for PA11 material was used for this step. This inovlves calibrating the load displcement curves for

simulated specienmen without hole with the obtained experimental data. As a result, in fig 8 the calibrated experimental & simulted data can be seen are in excellent agreement.

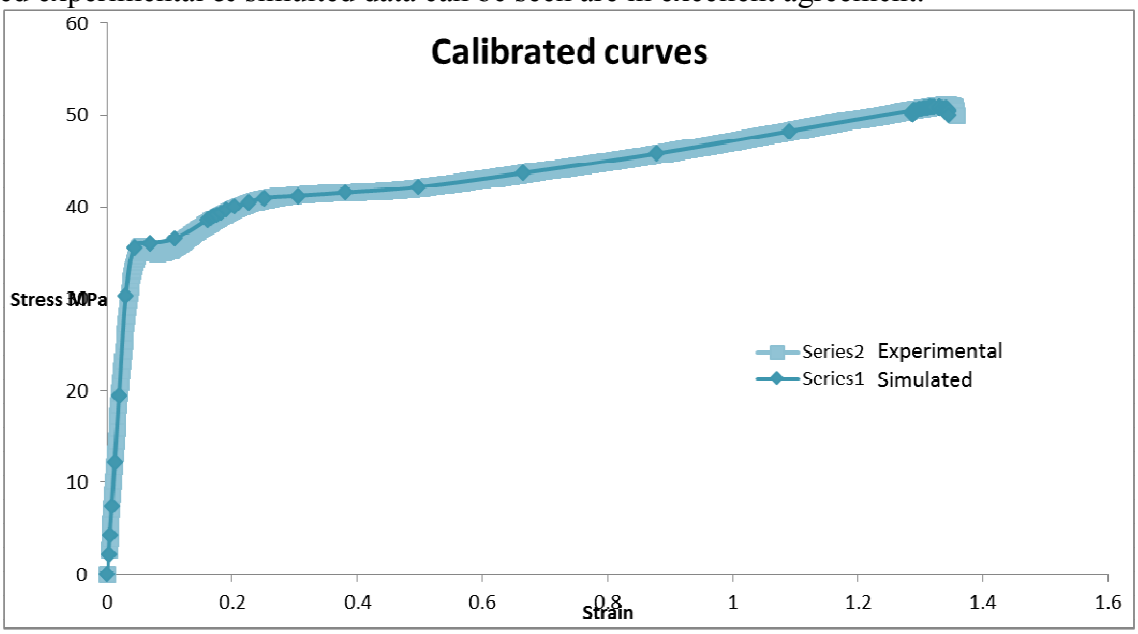

Fig. 8 Calibrated Stress strain curves for PA11

The next step involves validating this model for an impinged specimen i.e. specimen with a hole. The speicmen with smallest hole (1/8 in.) was chosen to begin with. From fig. 9, comaprison was drawn with the results from DIC and simulation. As seen in fig. 9, the max local strain that could be measured by DIC was 0.635 , the simulated results indicate local strain of 0.699 covering the similar area around hole as 0.635 in DIC analysis. So, there is a difference of about 10% between the expeimental and simulated local strain values.

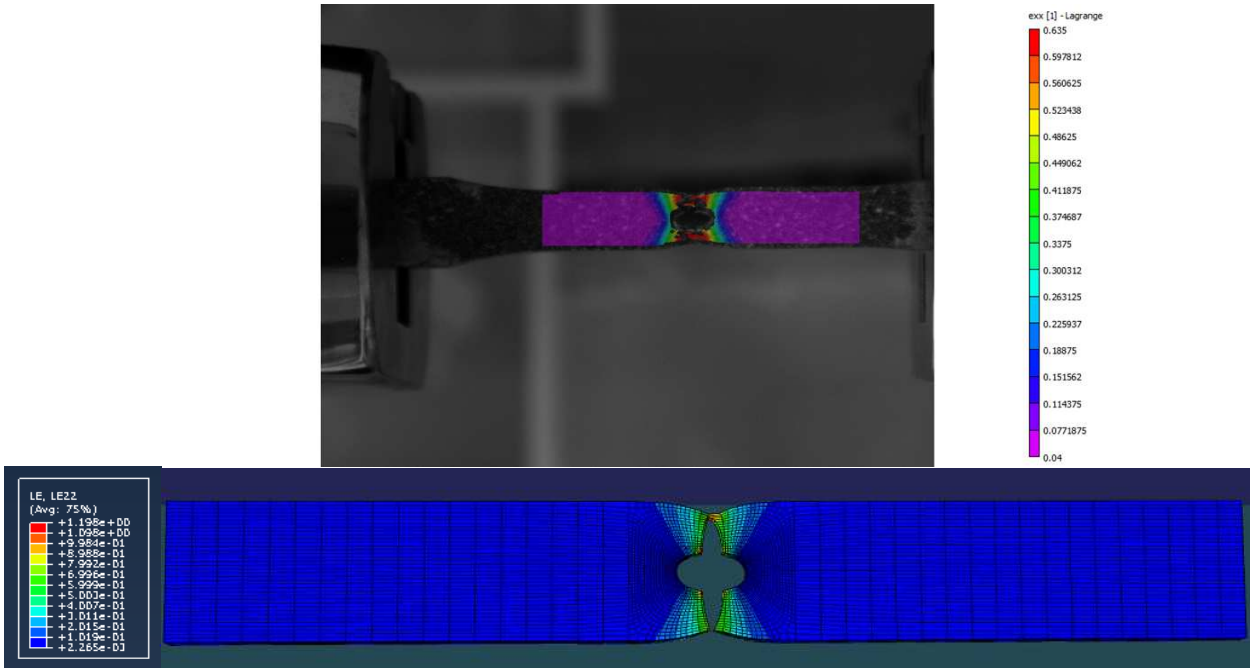

Fig. 9 Comparison between the DIC & simulation strain values

From the graph shown in fig. 10, the simulated curve traces the experimental curve for most of the time with similar elastic portion and peak load at around 301 lbf. However, there are some places where difference are seen indicating further need to fine tune the material modelling data. The difference in the fracture strain values of simulated & experimental results is around 5.88%. Further, the numerical

simulations are being carried out for all other impinged samples apart from PE samples whose experimental data are available.

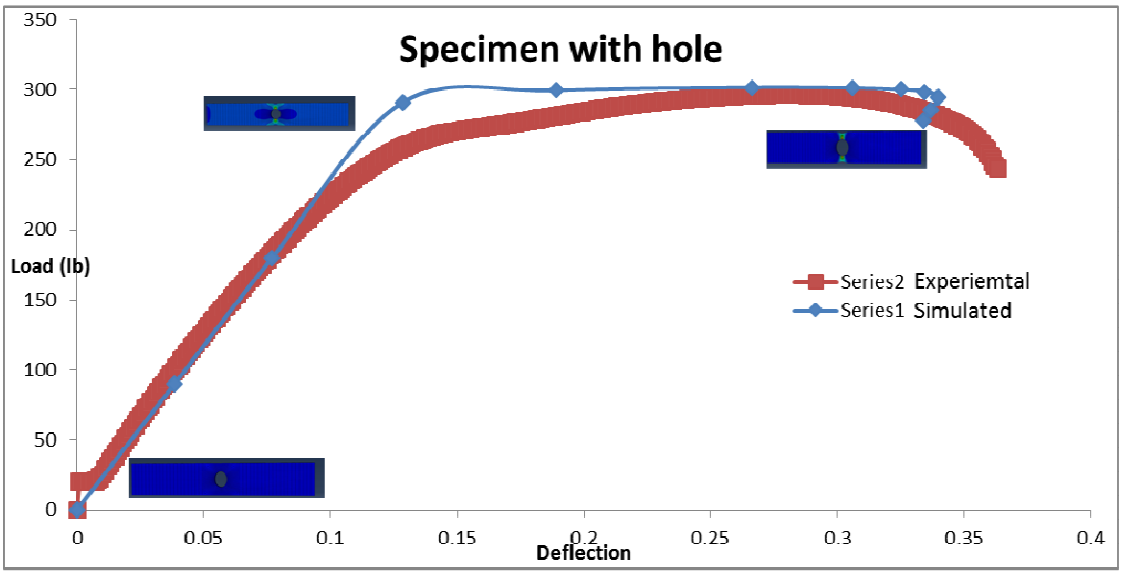

Fig. 10 Load Deflection of experimental & simulated specimen with hole

7.0 FUTURE WORK

- Numerical simulation for impinged PA 11 samples.
- Numerical simulation for impinged PE samples.
- Comprehensive comparison between PA11 & PE material & their suitability for pipeline application.

8.0 REFERENCES8

[1] Polyethylene (PE) | chemical compound. Retrieved December 6, 2015, from http://www.britannica.com/science/polyethylene

[2] O'Connor, C. (2012). Polyethylene Pipeline Systems - Avoiding The Pitfalls of Fusion Welding

[3] X. Q. Shi, Z. P. Wang, H. L. J. Pang, and X. R. Zhang, "Investigation of effect of temperature and strain rate on mechanical properties of underfill material by use of microtensile specimens," Polym. Test., vol. 21, no. 6, pp. 725–733, 2002.

[4] M. B. Saeed and M.-S. Zhan, "Effects of monomer structure and imidization degree on mechanical properties and viscoelastic behavior of thermoplastic polyimide films," Eur. Polym. J., vol. 42, no. 8, pp. 1844–1854, Aug. 2006.

[5] J. M. L. Reis, L. J. Pacheco, and H. S. da Costa Mattos, "Tensile behavior of post-consumer recycled high-density polyethylene at different strain rates," Polym. Test., vol. 32, no. 2, pp. 338–342, Apr. 2013.

[6] D. A. Şerban, G. Weber, L. Marşavina, V. V. Silberschmidt, and W. Hufenbach, "Tensile properties of semi-crystalline thermoplastic polymers: Effects of temperature and strain rates," Polym. Test., vol. 32, no. 2, pp. 413–425, Apr. 2013.

[7] M. R. Petersen, A. Chen, M. Roll, S. J. Jung, and M. Yossef, "Mechanical properties of fire-retardant glass fiber-reinforced polymer materials with Aluminum Tri-hydrate filler," Compos. Part B Eng.

[8] K. Dyamenahalli, A. Famili, and R. Shandas, "3 - Characterization of shape-memory polymers for biomedical applications," in Shape Memory Polymers for Biomedical Applications, L. Yahia, Ed. Woodhead Publishing, 2015, pp. 35–63.

Description of any Problems/Challenges

The project progress is satisfactory according to the schedule of tasks table. Good communications between the PIs, students and program director is well maintained. No technical challenges were identified in this quarter. The final report draft will be delivered in April according to the proposed project schedule.

(c) Planned Activities for the Next Quarter

Besides the planned activities mentioned in section (b), here are the future work for the next quarter:

FEKO and EFG simulation for PE and PA damage with experimental validation: A systematic study and imaging will be conducted in Q5. Experimental results will be analyzed and also validated by the simulation results. Raw data will also be delivered to ASU for further analysis.

XFEM simulation with multiphsics damage coupling: Following the previous kick offmeeting and phoen discussions, it was identified that other environmental damage may contribute to the final failure of pipeline systems, such as diffusion. ASU team is working on a general methodology to include this type of damage in the current simulation framework,

Final report drafting: The final report will be prepared as well as the project exit de-briefing meeting hosted by PHMSA.